Journal Pre-proof

Breakage of infant milk formula through three different processing methods and its influence on powder properties

Jie Han, John Fitzpatrick, Kevin Cronin, Valentyn Maidannyk, Song Miao

PII:	S0260-8774(20)30095-9
DOI:	https://doi.org/10.1016/j.jfoodeng.2020.109997
Reference:	JFOE 109997
To appear in:	*Journal of Food Engineering*
Received Date:	08 January 2020
Accepted Date:	23 February 2020

Please cite this article as: Jie Han, John Fitzpatrick, Kevin Cronin, Valentyn Maidannyk, Song Miao, Breakage of infant milk formula through three different processing methods and its influence on powder properties, *Journal of Food Engineering* (2020), https://doi.org/10.1016/j.jfoodeng.2020.109997

Breakage of infant milk formula through three different processing methods and its influence on powder properties

Jie Han [a,b], John Fitzpatrick [b], Kevin Cronin [b], Valentyn Maidannyk [a], Song Miao[a,*]

[a] Teagasc Food Research Centre, Moorepark, Fermoy, Co. Cork, Ireland

[b] Process & Chemical Engineering, School of Engineering, University College Cork, Cork, Ireland

* Corresponding author: Song.Miao@teagasc.ie

Abstract: Dairy powder breakage has always occurred during production and transportation though few studies on it have been published. This paper examines the breakage of infant formula using three different processing methods (laboratory high-speed mixing, lab-scale pneumatic conveying, and factory-scale blending) and the effect of breakage on powder properties. In both mixing and high-velocity pneumatic conveying, particles were broken into smaller entities and the particle size of samples significantly decreased. Particle breakage was accompanied by a significant decrease in porosity and increase in density and surface free fat. This in-turn decreased the rehydration properties of samples, especially for high-speed mixing, while breakage had only a small influence on powder flowability. By contrast, some agglomeration occurred during blending for short time in the blender and the particle size did not decrease (P>0.05) even for blending at longer time, thus, there were only minor impacts on physical and functional properties of powders.

Keywords: Dairy powder breakage; Physical characteristics; Rehydration properties; Flowability; Specific bulk volume; Powder compressibility

1. Introduction

The production of dairy powders is growing rapidly worldwide. Several physical characteristics, including particle size, density, porosity, morphology, surface, and adsorption properties, are important to powder functionalities (Bronlund and Paterson, 2004; Fitzpatrick et al., 2004; Fu et al., 2012). There are many factors influencing these properties, from composition, production processes, transportation, to storage conditions (Finney et al., 2002; Ji et al., 2016b; Langrish et al., 2006; Sharma et al., 2012). Currently, most studies on factors influencing dairy powder characteristics have mainly focused on the ingredients, the parameters during homogenization and spray drying, but ignored powder changes caused by mechanical forces. Particle breakage will occur after spray drying due to mechanical forces acting on the powder during the post-drying and transportation processes. There are very few published works on the breakage of dairy powders. Boiarkina et al. investigated the breakage of instant whole milk powder in two different industrial plants with different transport systems, i.e. a pneumatic conveying system, and a bucket elevator (Boiarkina et al., 2016).

Hanley investigated the disintegration of infant formula agglomerates with large particle sizes between 710 μm and 850 μm during pneumatic conveying (Hanley, 2011).

Particle breakage is the disintegration of powder particles caused by mechanical loads, such as impact, shear, and compression/crushing, which is the result of particle-particle and particle-equipment interactions (Aarseth, 2004; Zhao et al., 1999). Currently, research on particle breakage has mainly focused on the pharmaceutical industry, mining industry, catalysts chemical industry using numerical modeling combined with different types of single particle breakage tests (Deng and Davé, 2017; Dosta et al., 2016; Gupta et al., 2017; Gupta, 2017; Norazirah et al., 2016; Shan et al., 2018). There are three breakage mechanisms based on the resulting size distribution of child particles: fragmentation/damage, chipping/attrition, and fracture (Aarseth, 2004; Ghadiri and Zhang, 2002; Lawn and Swain, 1975). If the breakage is excessive, it can lead to a number of serious consequences including but not limited to an increase in dust generation (Kalman and Goder, 1998; Oveisi et al., 2013; Salman et al., 2002; Wu and Wu, 2017) and loss in functionality and product performance (Bemrose and Bridgwater, 1987; Boiarkina et al., 2016; Zumaeta et al., 2005). Specifically, fine dust produced may lead to air pollution and plugging of processing equipment, increased possibility of dust explosions, loss of product through the production of undersized particles. In addition, unwanted changes in bulk density may cause error in volumetric dosing processes, worsen wetting and dissolution properties, and influence the surface-sensitivity of catalytic particles. Particle size is an essential and important property for dairy powders (Li et al., 2016b). Thus, particle breakage is a problem that cannot be ignored in dairy powder production. However, only a few studies about dairy powder breakage have been published and none have investigated the dairy powder breakage patterns.

The objective of this study is to investigate the breakage of commercial agglomerated infant formula using three processing methods, lab-scale pneumatic conveying, laboratory high-speed mixing and factory-scale blending. At the same time, the influences of breakage on physical properties and functional properties (rehydration, powder flowability, and specific storage volume) of infant formula were investigated. The aim is to build a better understanding of dairy powder breakage and its influence.

2. Material and methods

2.1 Materials

Two batches of Cow and Gate "follow on milk stage 2" infant milk formulas were purchased from a local pharmacy (Cork, Ireland) to complete all the experiments. The nominal composition was 56.4% lactose, 20.4% fat, and 9.5% protein in this infant formula.

2.2 Equipment and powder breakage sample preparation

An isometric view of the lab-scale pneumatic conveyor (Hanley, 2011) and photos of the inside of the laboratory high-speed mixer (Waring, USA) and the factory-scale blender (Forberg, F-20, Norway) are presented in Figure 1. Samples were placed in the mixer operated at 22,000 rpm for three different durations of 1 min, 2 min, and 7 min (termed HSM1, HSM2, and HSM7). Other samples were placed in the Forberg blender for the duration of 15 min, 30 min, and 70 min (termed FB15, FB30, and FB70). The processing capacities for mixer and blender were 100 g and 1,600 g, respectively. Samples just covered the blade of the mixer and the level of the powder was in the middle of the blade in the blender.

The second batch of infant formula samples was blown through the pneumatic conveyor with an air velocity of 40 m/s and 50 m/s (termed PC40 and PC50) and feeding rate of 3.0 g/s. The diameter of the conveyor was constant at 25 mm, except for a 50 mm diameter terminal section (length was 150 mm). There were two horizontal sections linked to a vertical section (length was 960 mm) by two 90º bends (bend radii was 300 mm). The pressure of the compressed air was controlled to provide different air velocities which were measured with an airflow meter (Nixon NL/MIN AIR @ 7 bar'G 1.293kg/m3 20ºC) after the vertical section. Samples were poured into the air stream using a funnel and collected into a 10 L powder capture with a filter on the top of the capture in order to let the compressed air come out.

It should be noted that the samples used in this study were a packaged product that had most likely already undergone breakage during its handling from spray drying through to packing and thus this powder was more resistant to breakage than the original spray-dried

powder. Therefore, the processing conditions described above are relatively severe and were selected to ensure breakage could be expected.

2.3 Particle size distribution and specific surface area

The particle size distribution (PSD) and specific surface area (SSA) were measured by laser light scattering using a Malvern Mastersizer 3000 (Malvern Instruments Ltd., Worcestershire, UK). Compressed air at 0.2 bar was used to transport and disperse powders through the optical cell. Measurements were performed in triplicate.

2.4 Bulk density, particle density, and porosity

Loose bulk density (ρ_b) and tapped (100 taps) bulk density (ρ_{tapped}) of all samples were measured using a Jolting volumeter (Funke Gerber, Berlin, Germany) as per analytical methods (Niro, 2006b) from GEA Niro (Gesellschaft für Entstaubungsanlagen, Germany). Particle density (ρ_p) was measured based on GEA Niro (Niro, 2006d) using a Gas Pycnometer (Accupyc II 1340 Gas Pycnometer, Micromeritics Instrument Corporation, USA). The interparticle porosity (ε) is defined as the fraction of air or void space in the tapped bulk volume (Sharma et al., 2012) and was evaluated from Eq. (1).

$$\epsilon = 1 - \frac{\rho_{tapped}}{\rho_p} \qquad \text{Eq. (1)}$$

2.5 Scanning electron microscopy (SEM)

The SEM (Zeiss-Supra 40 VP/Gemini Column, Carl Zeiss, Germany) was employed to observe the morphology of the samples at 2.00 kV. Samples were mounted on carbon adhesive discs attached to SEM specimen stubs and coated with gold ions in a sputter coater (K575X Sputter Coater, Quorum Technologies, UK).

2.6 Surface free fat content

The surface free fat (SFF) content of milk powder was measured as per GEA Niro (Niro, 2006c), which is based on the extraction of the fat on the surface of particles.

2.7 Rehydration properties

2 2.7.1 Wettability - contact angle

3 Dynamic contact angle was used to quantify the wetting process. This was monitored by an
4 optical Tensiometer (Attention Theta, Biolin Scientific Ltd., Espoo, Finland) using the sessile
5 drop spread wetting procedure (Ji et al., 2016a). A powder bed with a smooth surface was
6 formed by passing a leveler across the surface. A set volume of 10 mL deionized water
7 droplet was gently dropped onto the surface of the powder bed at room temperature. The
8 contact angle was recorded as a function of penetrating time which had a total duration of 600
9 s. Measurements were repeated five times.

10 2.7.2 Dispersibility – dispersibility index

11 The dispersibility index (*DI*) of samples was measured as per GEA (Niro, 2006a). The use
12 of *DI* is the traditional standard method to measure the percentage of dry matter that passes
13 through a sieve (180 μm) after mixing for a short time. All the measurements were repeated
14 three times. In this study, 25 g infant formula sample was added into a 600 mL beaker with
15 250 mL deionized water at 37 ºC and then mixed vigorously with a spatula for exactly 20 s
16 making 20 full strokes along the diameter of the beaker in both directions. The reconstituted
17 samples were then poured onto the 180 μm sieve and the samples that passed through the
18 sieve were collected for further measurement of dry matter content. The *DI* was calculated as
19 Eq. (2):

20 $$DI = \frac{W_d \times (100 + W)}{w \times \frac{100 - W_m}{100}} \quad \text{Eq. (2)}$$

21 where w is the weight of the sample, W_d (%, w/w) is the dry matter, W_m (%, w/w) is the free
22 moisture content of the powder. All the measurements were repeated three times.

23 2.8 Powder flowability - flow function test

24 The flowability of the powder samples was assessed by measuring their flow function.
25 Powder flow functions were quantified and analyzed by the powder flow tester (PFT)
26 (Brookfield Engineering Laboratories, Inc., Middleboro, MA, USA) using the standard flow
27 function test. Samples were filled into the aluminum trough (with the internal diameter 15.2
28 cm) of the annular shear cell at room temperature. The axial and torsional speeds for the PFT
29 were 1.0 mm/s and 1 rev/h, respectively. The uniaxial normal stresses applied were between
30 0.2 and 4.8 kPa.

31 2.9 Bulk density under consolidation

Bulk density and its variation under consolidation load is an important property of a powder. The PFT was used to measure the bulk density of the powders at the consolidation stresses used in section 2.8 above. The compressibility index (*CI*) indicates the extent to which the volume of a powder sample changes under a compressive load and it is used for analyzing the compressibility of powders during storage (Bhandari et al., 2013; Ji et al., 2017). The *CI* was calculated from Eq. (3):

$$CI(\%) = \frac{\rho_c - \rho_b}{\rho_c} \times 100 \quad \text{Eq. (3)}$$

where ρ_b is the loose bulk density without compressing; ρ_c is the compressed bulk density at 4.838 kPa major principle consolidation stress. All the measurements were repeated in triplicate.

2.10 Statistical analysis

Results were expressed as mean ± standard deviation (SD). One-way analysis of variance (ANOVA), followed by Turkey's test, was used to determine the significant differences (SPSS, IBM, USA). A significance level of $P < 0.05$ was used throughout the study.

3. Results and discussion

Breakage directly affects powder particle size and other physical properties, and as a consequence, may influence its functional properties, such as the ability to rehydrate, flow properties and specific storage volume.

3.1 Powder physical properties

3.1.1 Particle size and specific surface area

The particle size and SSA of samples are shown in Figure 2 and Table 1, respectively. After breakage, the particle size of PC and HSM samples was significantly smaller than that of control samples ($P<0.05$). Meanwhile, with the increase of treatment time (in the HSM group) or air velocities (in the PC group), the particle size decreased gradually. For the pneumatic conveyor, particle size fell from 126 μm to 117.3 μm (at a conveying speed of 40 m/s) and to 109.3 μm for a speed of 50 m/s. For the high-speed mixer, breakage was significant too with particle size falling from 143 μm progressively to 65.4 μm for lengthening mixing times. The significant differences in SSA were also found in those two groups ($P<0.05$) and SSA increased with the decrease of particle size. The SSA was doubled after breakage for 7 min by the high-speed mixer. By contrast, powder in the Forberg blender was relatively unaffected by breakage with marginal changes in mean size for different

blending times (P>0.05); particle size increased slightly for short blending times but then fell back at longer times.

In order to further investigate the breakage patterns of samples during the three processing methods, the percentage change in three different sizes, D_{10}, D_{50} and D_{90} for each system and condition and PSD plots were analyzed and shown in Figure 3 and Figure 4, respectively. The HSM and PC samples had much higher decreased ratios than FB samples, which illustrates that particles of HSM and PC group disintegrated much more than the FB group of particles. In pneumatic conveying, there was a similar decrease in all these sizes; a 5% decrease at 40 m/s and a 13% decrease at 50 m/s. This implies that all particles broke proportionally and the dispersion in size remained approximately the same. For the mixer, longer mixing times produced increasingly larger changes in these three size points ranging from 14% at the shortest time to over 45% at the longest time and their PSD plots shifted towards smaller values. Meanwhile, for this device, the D_{10} size always experienced a larger decrease than the D_{50} and D_{90} (P<0.05), which means all particles were broken with the production of more fine particles. The breakage during mixing and pneumatic conveying is typically associated with high-magnitude loading conditions, where the stresses applied to the particle exceed the particle strength and generate free surface area (Kotzur et al., 2018). On the contrary for the Forberg blender, the D_{10}, D_{50} and D_{90} of FB15 and FB30 were slightly increased compared to their control sample. This result might be because some agglomeration occurred resulting in the decrease of fine particles and a slight increase of particle size.

Particle size is an important characteristic of dairy powder as it is closely related to many other characteristics, such as appearance, rehydration, flowability, and density (Fitzpatrick et al., 2004; Sharma et al., 2012). The SSA values might affect the water sorption behaviors as the large surface area of particles meant more area for water molecules to attach.

3.1.2 Bulk density, particle density, and porosity

The density and porosity values of samples are shown in Table 1. Powder bulk density is used for calculating the volumetric capacity of packing materials. It was shown that the bulk density of most broken samples significantly increased compared to control samples, and the porosity significantly decreased (P<0.05). After breakage, small particles that were broken from the original particles possibly filled void spaces between large particles, which caused the increase of the bulk density and the decrease of the porosity. The bulk density and porosity of some FB samples also changed (P<0.05), which suggests that blending did influence structure even though the particle size did not decrease.

Particle density is the mass per unit volume of a particle, excluding the open pores but including the closed pores (Sharma et al., 2012). After breakage, the particle density of PC and HSM samples increased (P<0.05). The SEM micrographs of some samples are shown in Figure 5. From micrographs, there were a lot of pores inside particles. Thus, the breakage did not only break solid bridges within agglomerated particles resulting in decreased particle size and increased bulk density, but also broke primary particles exposing internal stomata leading to the increase of the particle density.

3.1.3 Surface free fat

The surface free fat (SFF) content of samples is shown in Table 1. After breakage, the SFF of some samples were significantly increased (P<0.05), especially for HSM samples, PC50 and FB70. Meanwhile, the SFF increased gradually with the increase of the processing time. HSM7 had the highest SFF, 1.88±0.04%, which was four times more than the control sample. Powder particles generally consist of a continuous mass of amorphous lactose and other components in which fat globules and proteins are embedded (Sharma et al., 2012). The unprotected fat on particles covers the outermost surface and, beneath it fat bound to protein or proteins is present (Kim et al., 2003; Nijdam and Langrish, 2006). Particle breakage produced more surface area and liberated more free fat, which resulted in an increase of the SFF. The increase in SFF of the Forberg blender samples might be because the inter-particle contact was sufficient to break fat globules on the surface. At the same time, it might explain the small increases in particle size as the fat acts as a binder inducing some agglomeration. The increase of the SFF might affect the rehydration properties, especially for the wettability, as the SFF influences the surface hydrophobicity of powders.

3.2 Rehydration properties

3.2.1 Wettability - contact angles

Wettability is the ability of particles to imbibe a liquid and overcome the surface tension between them based on the capillary force (Forny et al., 2011; Ji et al., 2015; Ji et al., 2016a; Richard et al., 2013). The contact angle is usually used as a primary parameter to indicate the degree of the wetting process with a small contact angle ($\theta < 90^{o}$) representing good wettability and a large angle ($\theta > 90^{o}$) corresponding to poor wettability (Yuan and Lee, 2013). It is important to monitor the change of contact angle until reaching an equilibrium angle to quantify the wettability of powders as wetting behavior is a dynamic procedure (Crowley et al., 2015). The penetrating time for water droplets to disappear and curves of contact angle as a function of penetrating time are shown in Figure 6. There was no significant difference in the penetrating time between FB samples, and water droplets were absorbed in 0.75 s. For

PC40 and PC50 samples, droplets took 1.94 and 2.95 s to disappear, respectively; while the PC0 sample took around 0.94 s. These significant differences(P<0.05) mean when the air velocity is high enough, pneumatic conveying samples have poorer wettability compared to the control sample. The HSM samples exhibited extremely poor wetting behaviors with penetration times of 4 s, 35 s, and 5 min for HSM1, HSM2, and HSM7, respectively. Figure 6B also showed that the changes in contact angles of PC and HSM samples were significantly slower than that of control samples. Thus, broken samples had poor wettability compared to control samples and as the degree of breakage increased, the wettability became worse.

There are two steps for the wetting process of powders. The first step is the replacement of gas by water so the interface of powder-gas is replaced by the interface of powder-water. Secondly, inward diffusion of the liquid occurs through the capillary structures of the porous powder particle (Yuan and Lee, 2013). It is usually believed that wettability improves with larger particle size with higher bed porosity (Hogekamp and Schubert, 2003). The significant decrease of the particle size and porosity, as well as the increase of the SFF, especially for the HSM samples, is most likely the main reason for the poor wettability. Lower porosity with a small capillary radius between particles and greater surface hydrophobicity due to higher SFF inhibited water penetration into the powders, thus slowing down the wetting process.

3.2.2 Dispersibility - dispersibility index

Dispersibility is also an important step in the rehydration process, as it is necessary for particles to be dispersed into the liquid before dissolving (Galet et al., 2004; Goalard et al., 2006). Figure 7 illustrates the influence of breakage on the *DI* of samples. For PC and HSM samples, the *DI* significantly decreased compared to control samples and decreased gradually with the increase of treatment time. While, for FB samples, there was no significant difference between the *DI*. The substantial decrease of particle size and porosity, and increased SFF might be the reason for the deterioration of the dispersibility of broken samples by slowing down the penetration of water into the powder.

3.3 Flow properties

For spray-dried dairy powder, the flow properties are very important in handling and processing operations (Kim et al., 2005; Peleg, 1977). The measured powder flow functions are presented in Figure 8. The flow functions show that all powder samples were essentially easy-flowing. It also shows that breakage had only a small influence on the flow functions. For the PC and HSM samples, it shows that breakage resulted in a small reduction in powder flowability. However, the FB powders displayed the poorest flowability relative to the others, even though there was little or no breakage.

Flow properties of dairy powders depend on their composition, in particular surface composition and physical characteristics, such as particle size distribution, porosity, particle shape, surface properties, and water content (Crowley et al., 2014; Janjatović et al., 2012; Kim et al., 2005). The SFF of powders increased after breakage, which could be one of the reasons for the small decrease in powder flowability. SFF influences powder stickiness and liquid fat can form liquid bridges between individual particles reducing flowability (Kim et al., 2005; Peleg, 1977; Sharma et al., 2012). Furthermore, particle size decreased and bulk density increased after breakage, which meant more particle surface area was available for cohesive and frictional forces to resist flow. Thus powder flowability was reduced. However, overall, the powder flow functions showed that the powder breakage observed did not have a major impact on powder flowability.

3.4 Specific bulk volume and powder compressibility

The specific bulk volume and how it is influenced by consolidation is an important powder functionality, as it influences the storage volume required to store a given mass of powder. Furthermore, for infant formula, the specific bulk volume influences the size of product containers and the scoop volume requirement for the preparation of infant milk (Hanley, 2011; Li et al., 2016a). The loose specific bulk volume is presented in Table 2 (This is the inverse of loose bulk density). It shows that the breakage occurring during pneumatic conveying and high-speed mixing significantly reduced the specific bulk volume requirement by about 3 to 11%. It also shows little or no reduction in specific bulk volume for the Forberg blender, as there was little or no breakage.

Figure 9 shows how bulk density varies for the different powder samples under consolidation. As expected, consolidation resulted in higher bulk densities for all the samples. Like the loose powder case, Figure 9 shows that breakage resulted in higher bulk densities for all consolidations. This shows that breakage resulted in reduced specific bulk volume requirements under consolidations tested.

The compressibility index (*CI*) was calculated using the bulk density data (at 4.838 kPa major principle consolidation stress). A high *CI* indicates the potential for high compressibility of powders during storage or transportation (Crowley et al., 2014). Table 2 presents the *CI* of the different powder samples, which shows values mainly in the range of 26 to 29%, due to increases in bulk density during consolidation. Table 2 also shows that there was no significant relationship between breakage and the *CI* of the samples, which means that breakage had no influence on the compressibility of samples, even with the significant decrease in particle size and porosity. This is in-part due to the definition of *CI* in

Eq. (3). Even though the compressed bulk density (ρ_c) is higher with greater breakage, the loose bulk density (ρ_b) is also higher, resulting in no clear relationship between breakage and *CI*.

4. Conclusion

A study was performed on the particle breakage of commercial infant formula during three different processing methods (lab-scale pneumatic conveyor, laboratory high-speed mixer and Forberg blender), and how the breakage influenced the powder physical properties and functional properties (rehydration, flowability, and storage volume). The Forberg blender had a relatively small effect on particle size, even for very long blending times, but it did cause a gradual increase in SFF content, which may explain the small increases in average particle size observed. There were only minor impacts on the physical and functional properties of powder blended in the Forberg blender due to the minor changes in particle size.

Significant particle breakage occurred in the pneumatic conveyor and the high-speed laboratory mixer, and the longer or the more intense the processing, the greater was the breakage. Particle breakage was accompanied by an increase in SFF content and bulk density. This in-turn impacted on powder rehydration in particular. Particle breakage caused a major reduction in powder wettability, especially for the high-speed mixer at longer times where much breakage occurred. This was most likely due to the combined effect of increased SFF and smaller particle size. These results emphasize the importance of controlling breakage levels in processing to maintain rehydration properties. Particle breakage increased bulk density, which in-turn reduced specific bulk storage volume by about 3 to 11%. Breakage in the high-speed mixer and pneumatic conveyor did not have a major impact on powder flowability, where there was only a minor negative impact observed.

Acknowledgment

This work was supported financially by the Teagasc, Agriculture and Food Development Authority under the project MDDT 0153 entitled ‘Powder breakage and functionality of dairy powders’. Ms. Han was funded under the Teagasc Walsh Fellowship Scheme.

Reference

Aarseth, K.A., (2004). Attrition of Feed Pellets during Pneumatic Conveying: the Influence of Velocity and Bend Radius. Biosystems Engineering 89(2), 197-213.

Bemrose, C.R., Bridgwater, J., (1987). A review of attrition and attrition test methods. Powder Technology 49(2), 97-126.

Bhandari, B.R., Bansal, N., Zhang, M., Schuck, P., (2013). *Handbook of food powders: Processes and properties*. Elsevier.

Boiarkina, I., Sang, C., Depree, N., Prince-Pike, A., Yu, W., Wilson, D.I., Young, B.R., (2016). The significance of powder breakdown during conveying within industrial milk powder plants. Advanced Powder Technology 27(6), 2363-2369.
Bronlund, J., Paterson, T., (2004). Moisture sorption isotherms for crystalline, amorphous and predominantly crystalline lactose powders. International Dairy Journal 14(3), 247-254.
Crowley, S.V., Desautel, B., Gazi, I., Kelly, A.L., Huppertz, T., O'Mahony, J.A., (2015). Rehydration characteristics of milk protein concentrate powders. Journal of Food Engineering 149, 105-113.
Crowley, S.V., Gazi, I., Kelly, A.L., Huppertz, T., O'Mahony, J.A., (2014). Influence of protein concentration on the physical characteristics and flow properties of milk protein concentrate powders. Journal of Food Engineering 135, 31-38.
Deng, X., Davé, R.N., (2017). Breakage of fractal agglomerates. Chemical Engineering Science 161, 117-126.
Dosta, M., Dale, S., Antonyuk, S., Wassgren, C., Heinrich, S., Litster, J.D., (2016). Numerical and experimental analysis of influence of granule microstructure on its compression breakage. Powder Technology 299, 87-97.
Finney, J., Buffo, R., Reineccius, G.A., (2002). Effects of Type of Atomization and Processing Temperatures on the Physical Properties and Stability of Spray-Dried Flavors. Journal of Food Science 67(3), 1108-1114.
Fitzpatrick, J.J., Iqbal, T., Delaney, C., Twomey, T., Keogh, M.K., (2004). Effect of powder properties and storage conditions on the flowability of milk powders with different fat contents. Journal of Food Engineering 64(4), 435-444.
Forny, L., Marabi, A., Palzer, S., (2011). Wetting, disintegration and dissolution of agglomerated water soluble powders. Powder Technology 206(1), 72-78.
Fu, X., Huck, D., Makein, L., Armstrong, B., Willen, U., Freeman, T., (2012). Effect of particle shape and size on flow properties of lactose powders. Particuology 10(2), 203-208.
Galet, L., Vu, T.O., Oulahna, D., Fages, J., (2004). The Wetting Behaviour and Dispersion Rate of Cocoa Powder in Water. Food and Bioproducts Processing 82(4), 298-303.
Ghadiri, M., Zhang, Z., (2002). Impact attrition of particulate solids. Part 1: A theoretical model of chipping. Chemical Engineering Science 57(17), 3659-3669.
Goalard, C., Samimi, A., Galet, L., Dodds, J.A., Ghadiri, M., (2006). Characterization of the Dispersion Behavior of Powders in Liquids. Particle & Particle Systems Characterization 23(2), 154-158.
Gupta, V., Sun, X., Xu, W., Sarv, H., Farzan, H., (2017). A discrete element method-based approach to predict the breakage of coal. Advanced Powder Technology 28(10), 2665-2677.
Gupta, V.K., (2017). Effect of size distribution of the particulate material on the specific breakage rate of particles in dry ball milling. Powder Technology 305, 714-722.
Hanley, K.J., (2011). Experimental quantification and modelling of attrition of infant formulae, *Department of Process and Chemical Engineering*. University College Cork, Cork, Ireland.
Hogekamp, S., Schubert, H., (2003). Rehydration of Food Powders. Food Science and Technology International 9(3), 223-235.
Janjatović, D., Benković, M., Srečec, S., Ježek, D., Špoljarić, I., Bauman, I., (2012). Assessment of powder flow characteristics in incoherent soup concentrates. Advanced Powder Technology 23(5), 620-631.
Ji, J., Cronin, K., Fitzpatrick, J., Fenelon, M., Miao, S., (2015). Effects of fluid bed agglomeration on the structure modification and reconstitution behaviour of milk protein isolate powders. Journal of Food Engineering 167, 175-182.
Ji, J., Fitzpatrick, J., Cronin, K., Crean, A., Miao, S., (2016a). Assessment of measurement characteristics for rehydration of milk protein based powders. Food Hydrocolloids 54, 151-161.

285 Ji, J., Fitzpatrick, J., Cronin, K., Fenelon, M.A., Miao, S., (2017). The effects of fluidised bed
286 and high shear mixer granulation processes on water adsorption and flow properties of
287 milk protein isolate powder. Journal of Food Engineering 192, 19-27.
288 Ji, J., Fitzpatrick, J., Cronin, K., Maguire, P., Zhang, H., Miao, S., (2016b). Rehydration
289 behaviours of high protein dairy powders: The influence of agglomeration on wettability,
290 dispersibility and solubility. Food Hydrocolloids 58, 194-203.
291 Kalman, H., Goder, D., (1998). Design criteria for particle attrition. Advanced Powder
292 Technology 9(2), 153-167.
293 Kim, E.H.J., Chen, X.D., Pearce, D., (2005). Effect of surface composition on the flowability
294 of industrial spray-dried dairy powders. Colloids and Surfaces B: Biointerfaces 46(3),
295 182-187.
296 Kim, E.H.J., Dong Chen, X., Pearce, D., (2003). On the Mechanisms of Surface Formation
297 and the Surface Compositions of Industrial Milk Powders. Drying Technology 21(2),
298 265-278.
299 Kotzur, B.A., Berry, R.J., Zigan, S., García-Triñanes, P., Bradley, M.S.A., (2018). Particle
300 attrition mechanisms, their characterisation, and application to horizontal lean phase
301 pneumatic conveying systems: A review. Powder Technology 334, 76-105.
302 Langrish, T.A.G., Marquez, N., Kota, K., (2006). An Investigation and Quantitative
303 Assessment of Particle Shape in Milk Powders from a Laboratory-Scale Spray Dryer.
304 Drying Technology 24(12), 1619-1630.
305 Lawn, B.R., Swain, M.V., (1975). Microfracture beneath point indentations in brittle solids.
306 Journal of Materials Science 10(1), 113-122.
307 Li, R., Roos, Y.H., Miao, S., (2016a). Influence of pre-crystallisation and water plasticization
308 on flow properties of lactose/WPI solids systems. Powder Technology 294, 365-372.
309 Li, R., Roos, Y.H., Miao, S., (2016b). Roles of particle size on physical and mechanical
310 properties of dairy model solids. Journal of Food Engineering 173, 69-75.
311 Nijdam, J.J., Langrish, T.A.G., (2006). The effect of surface composition on the functional
312 properties of milk powders. Journal of Food Engineering 77(4), 919-925.
313 Niro, G., (2006a). A 6 a - Powder Dispersibility. GEA Process Engineering A/S, Gladsaxevej,
314 Denmark,.
315 Niro, G., (2006b). A2a - Powder Bulk Density. GEA Process Engineering A/S, Gladsaxevej,
316 Denmark,.
317 Niro, G., (2006c). A10a - Surface Free Fat of Powder. GEA Process Engineering A/S,
318 Gladsaxevej, Denmark,.
319 Niro, G., (2006d). A11c - Particle Density, Occluded Air and Interstitial Air by Air
320 Pycnometer. GEA Process Engineering A/S, Gladsaxevej, Denmark,.
321 Norazirah, A., Fuad, S.H.S., Hazizan, M.H.M., (2016). The Effect of Size and Shape on
322 Breakage Characteristic of Mineral. Procedia Chemistry 19, 702-708.
323 Oveisi, E., Lau, A., Sokhansanj, S., Lim, C.J., Bi, X., Larsson, S.H., Melin, S., (2013).
324 Breakage behavior of wood pellets due to free fall. Powder Technology 235, 493-499.
325 Peleg, M., (1977). FLOWABILITY OF FOOD POWDERS AND METHODS FOR ITS
326 EVALUATION — A REVIEW. Journal of Food Process Engineering 1(4), 303-328.
327 Richard, B., Le Page, J.F., Schuck, P., Andre, C., Jeantet, R., Delaplace, G., (2013). Towards
328 a better control of dairy powder rehydration processes. International Dairy Journal 31(1),
329 18-28.
330 Salman, A.D., Hounslow, M.J., Verba, A., (2002). Particle fragmentation in dilute phase
331 pneumatic conveying. Powder Technology 126(2), 109-115.
332 Shan, J., Xu, S., Liu, Y., Zhou, L., Wang, P., (2018). Dynamic breakage of glass sphere
333 subjected to impact loading. Powder Technology 330, 317-329.
334 Sharma, A., Jana, A.H., Chavan, R.S., (2012). Functionality of Milk Powders and Milk-Based
335 Powders for End Use Applications—A Review. Comprehensive Reviews in Food
336 Science and Food Safety 11(5), 518-528.
337 Wu, F., Wu, D., (2017). Attrition resistances and mechanisms of three types of FCC catalysts.
338 Powder Technology 305, 289-296.

339 Yuan, Y., Lee, T.R., (2013). Contact angle and wetting properties, *Surface science techniques*.
340 Springer, pp. 3-34.
341 Zhao, R., Goodwin, J.G., Oukaci, R., (1999). Attrition assessment for slurry bubble column
342 reactor catalysts. Applied Catalysis A: General 189(1), 99-116.
343 Zumaeta, N., Cartland-Glover, G.M., Heffernan, S.P., Byrne, E.P., Fitzpatrick, J.J., (2005).
344 Breakage model development and application with CFD for predicting breakage of whey
345 protein precipitate particles. Chemical Engineering Science 60(13), 3443-3452.

Jie Han: Conceptualization, Methodology, Writing - original draft, Data curation.

John Fitzpatrick: Supervision, writing - review & editing.

Kevin Cronin: Supervision, Writing - review & editing.

Valentyn Maidannyk: Investigation.

Song Miao: Supervision, Conceptualization, Writing - review & editing, Funding acquisition, Project administration, Investigation.

Declaration of interests

☒ The authors declare that they have no known competing financial interests or personal relationships that could have appeared to influence the work reported in this paper.

☐The authors declare the following financial interests/personal relationships which may be considered as potential competing interests:

Song Miao

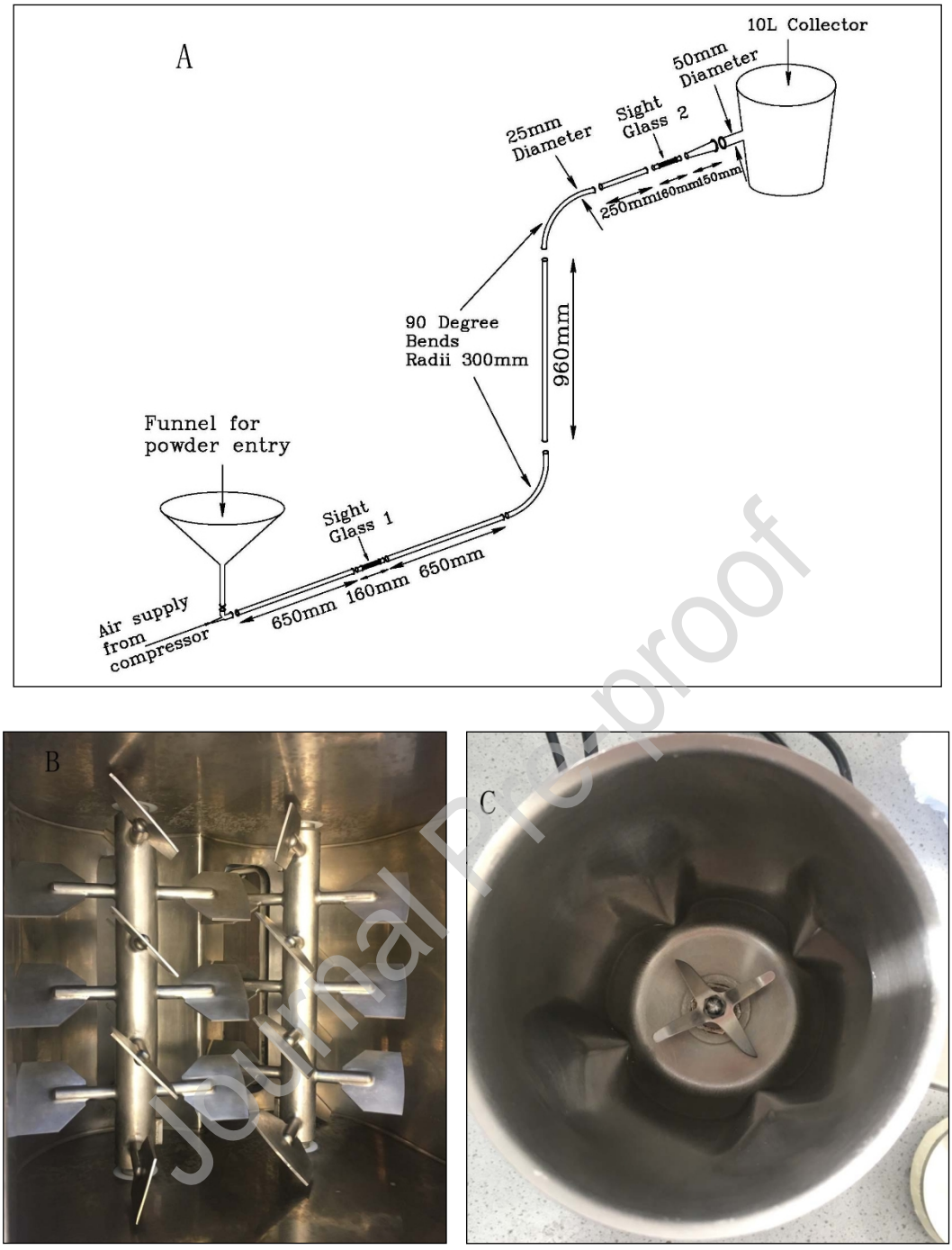

Figure1. An isometric view of the lab-scale pneumatic conveyor (A) and the inside of the Forberg blender (B) and laboratory high-speed mixer (C).

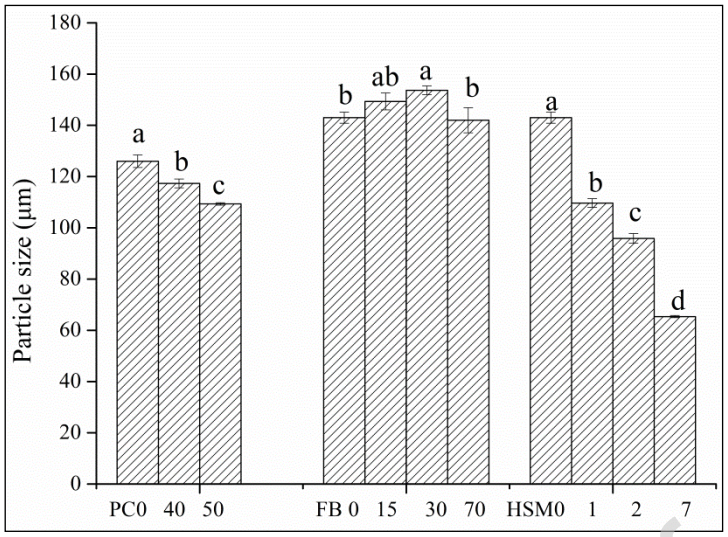

Figure 2. The particle size ([$D_{3,2}$]) of powder samples. PC: broken by pneumatic conveying under the air velocity of 40 m/s and 50 m/s. FB: broken by the Forberg blender for 15 min, 30 min, and 70 min. HSM: broken by the laboratory high-speed mixer for 1 min, 2 min, and 7 min. Different a-d values within each group (PC, FB and HSM) are significantly different at $P<0.05$.

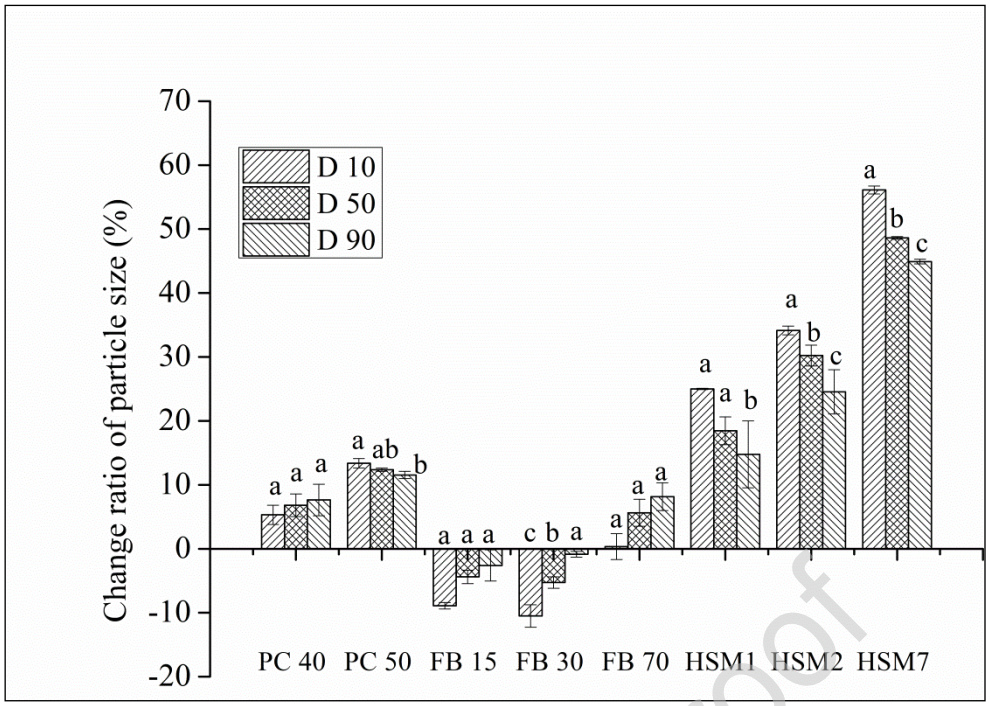

Figure 3. Percent decreases in different kinds of particle sizes (D_{10}, D_{50}, and D_{90}) of samples. D_{10}, D_{50}, and D_{90} mean 10%, 50%, and 90% of the sample are below this diameter, separately. PC: broken by pneumatic conveying under the air velocity of 40 m/s and 50 m/s. FB: broken by the Forberg blender for 15 min, 30 min, and 70 min. HSM: broken by the laboratory high-speed mixer for 1 min, 2 min, and 7 min. Different a-c values within each group (PC, FB and HSM) are significantly different at $P<0.05$.

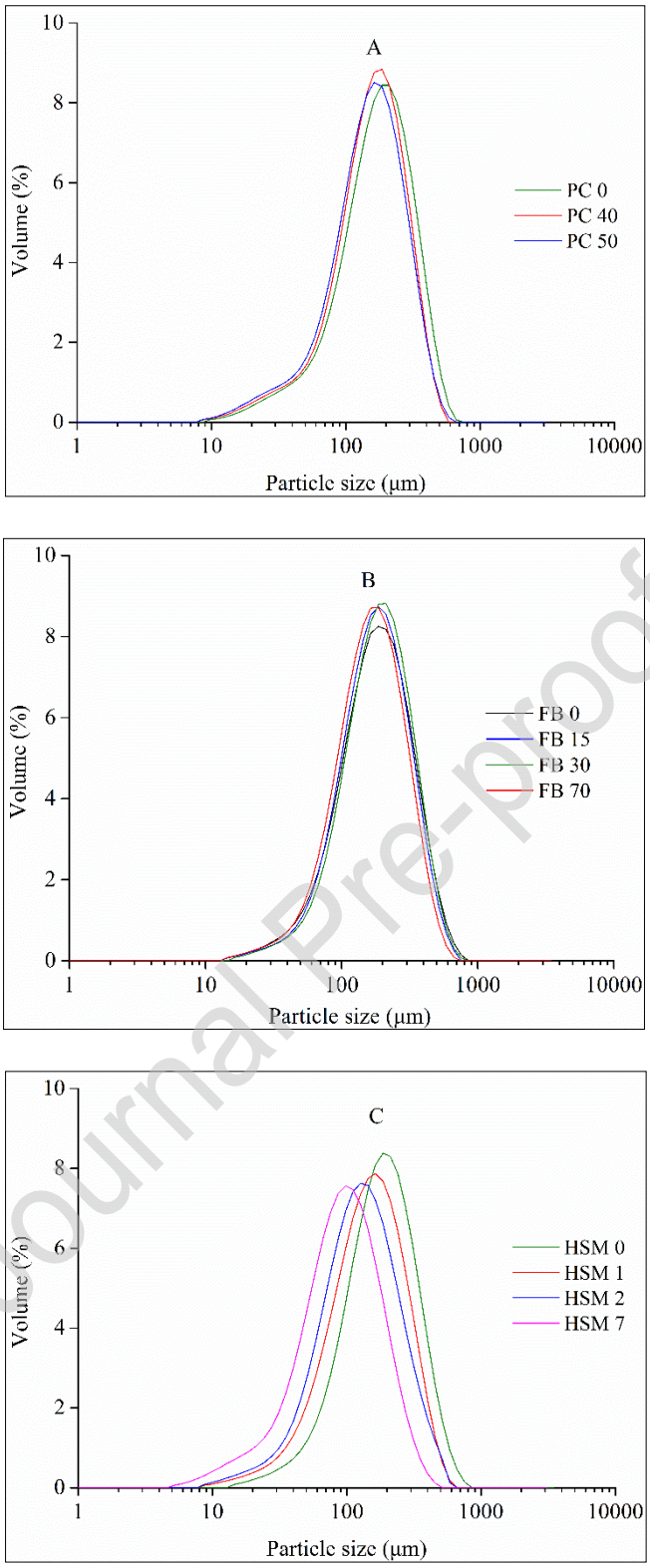

Figure 4. The particle size distribution plots of samples. PC: broken by pneumatic conveying under the air velocity of 40 m/s and 50 m/s; FB: broken by the Forberg blender for 15 min, 30 min, and 70 min. HSM: broken by the laboratory high-speed mixer for 1 min, 2 min, and 7 min.

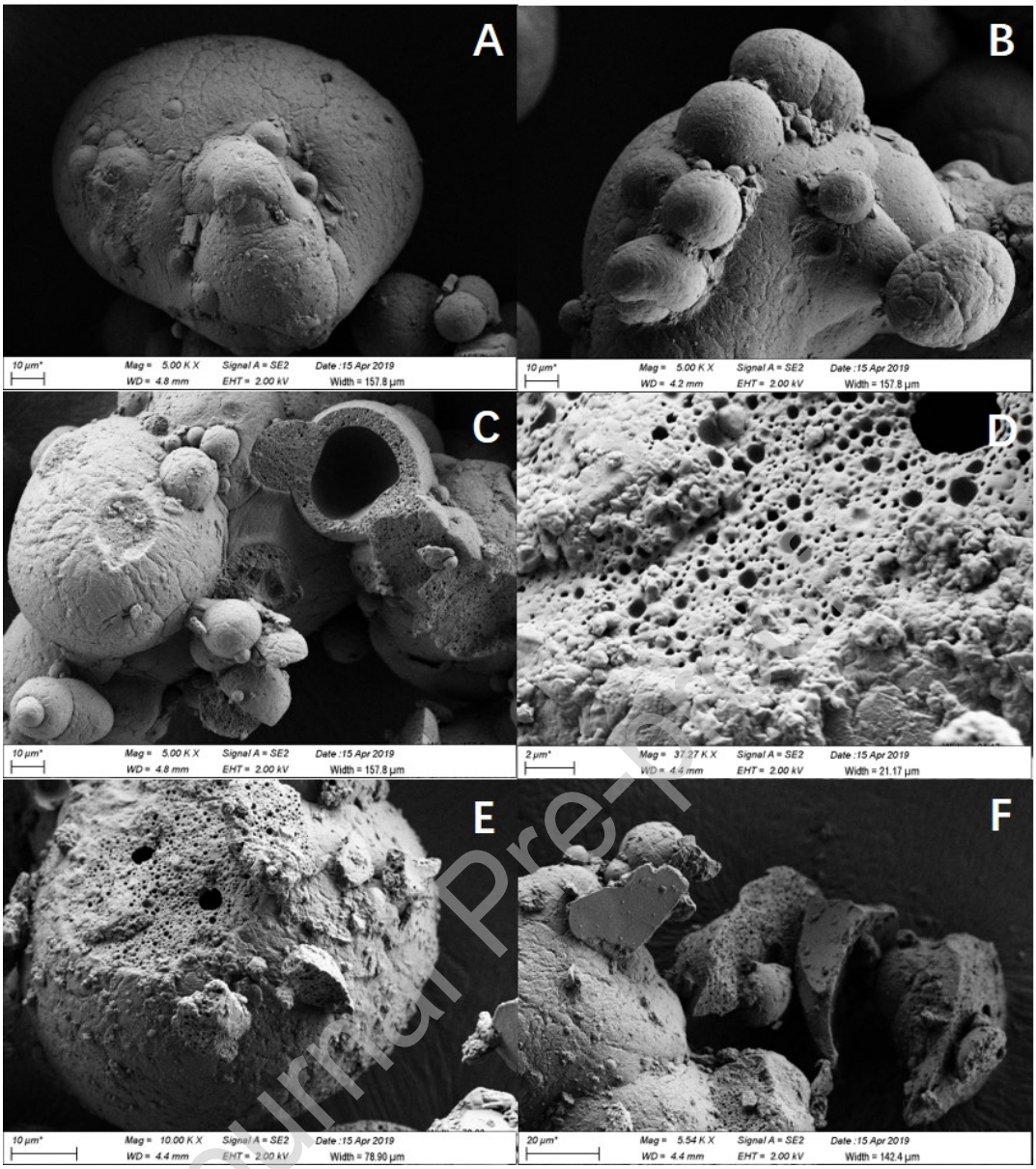

Figure 5. The SEM micrographs of control powder sample (A-B) and broken samples by the laboratory high-speed mixer for 7 min (C-F).

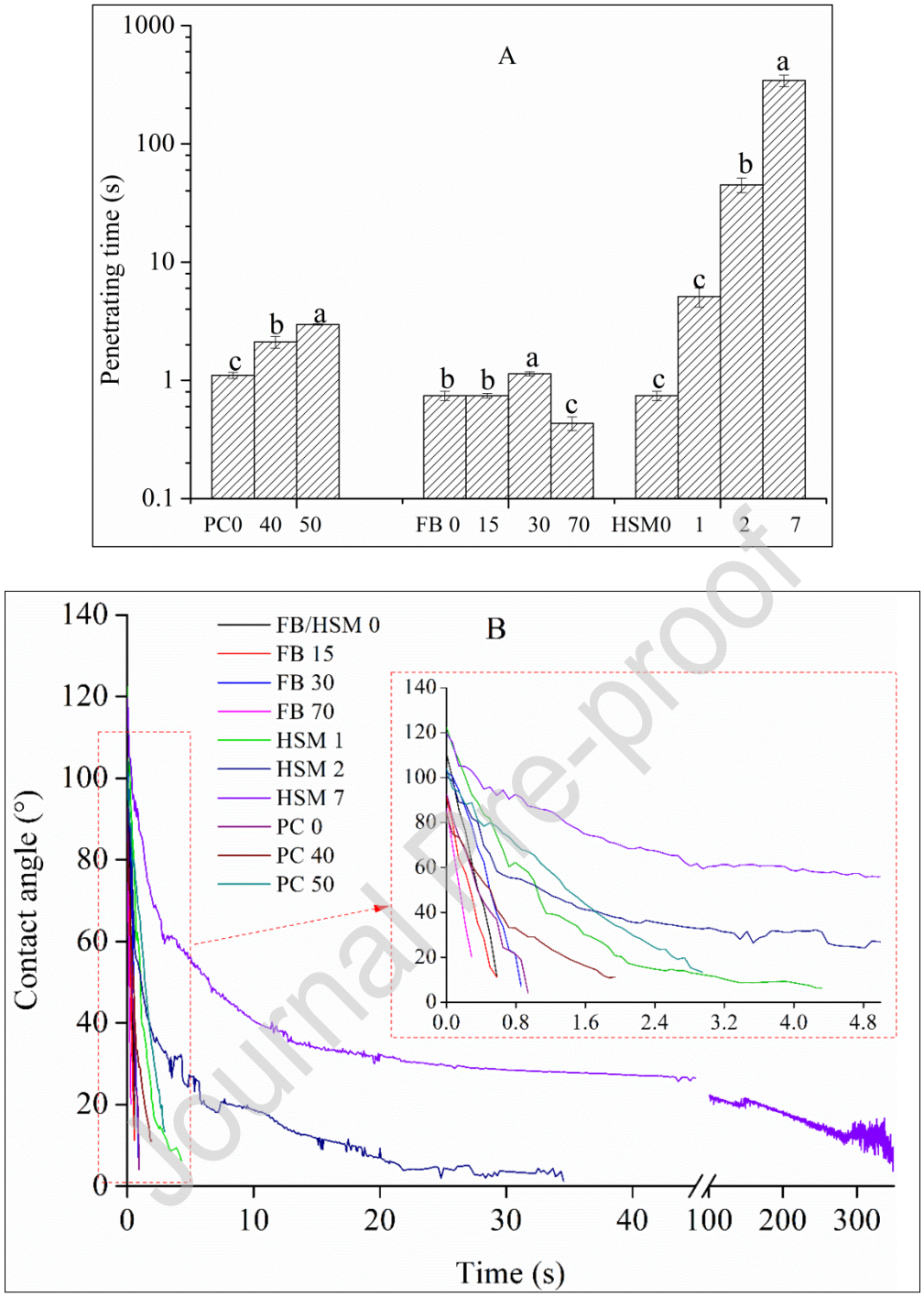

Figure 6. A: The penetrating time takes for water droplets to be absorbed. B: The change of contact angle as a function of penetrating time in approx. 20 ºC temperature. PC: broken by pneumatic conveying under the air velocity of 40 m/s and 50 m/s. FB: broken by the Forberg blender for 15 min, 30 min, and 70 min. HSM: broken by the laboratory high-speed mixer for 1 min, 2 min, and 7 min. Different a-c values within each group (PC, FB and HSM) are significantly different at $P<0.05$.

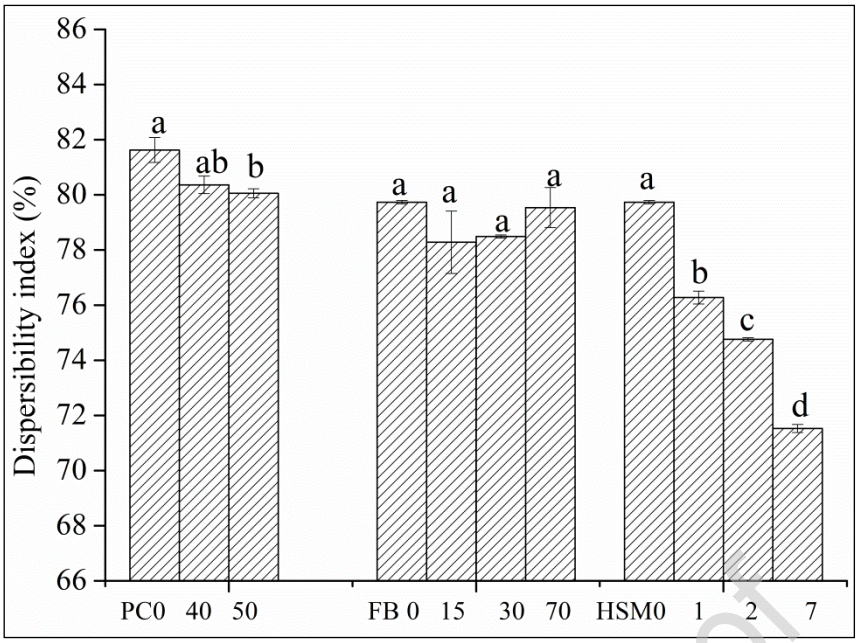

Figure 7. Dispersibility index for samples. PC: broken by pneumatic conveying under the air velocity of 40 m/s and 50 m/s. FB: broken by the Forberg blender for 15 min, 30 min, and 70 min. HSM: broken by the laboratory high-speed mixer for 1 min, 2 min, and 7 min. Different a-d values within each group (PC, FB and HSM) are significantly different at $P<0.05$.

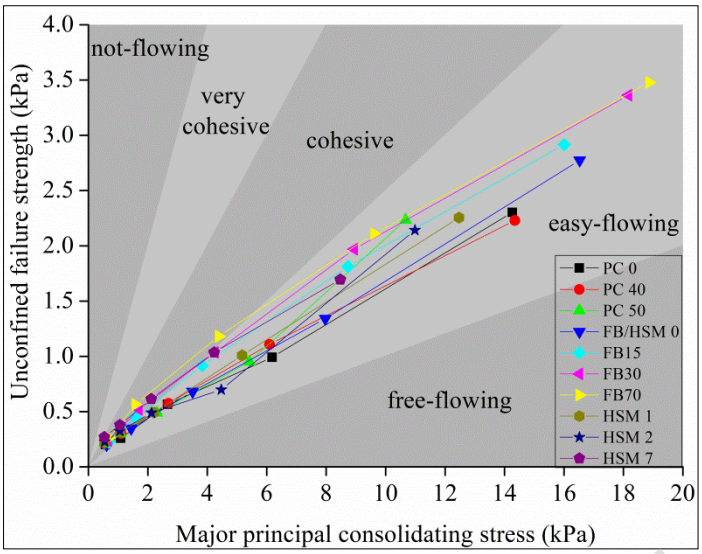

Figure 8. Unconfined strength as a function of major principal consolidating stress for infant formula samples. PC: broken by pneumatic conveying under the air velocity of 40 m/s and 50 m/s. FB: broken by the Forberg blender for 15 min, 30 min, and 70 min. HSM: broken by the laboratory high-speed mixer for 1 min, 2 min, and 7 min.

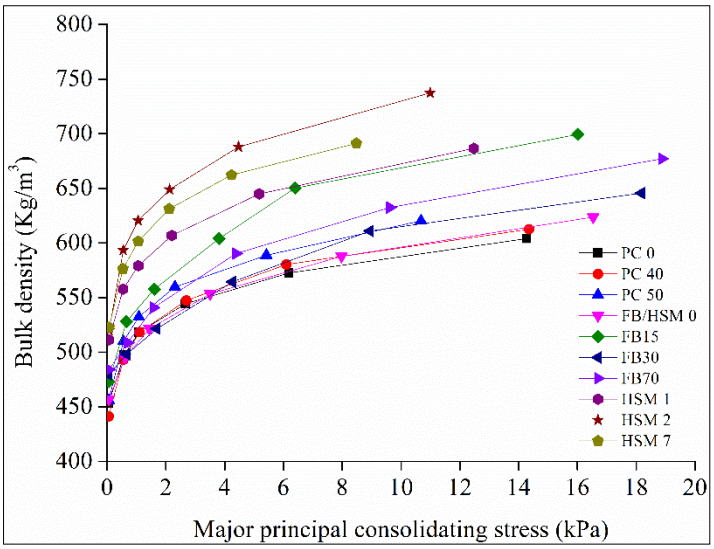

Figure 9. Bulk density as a function of major principal consolidating stress for infant formula samples. PC: broken by pneumatic conveying under the air velocity of 40 m/s and 50 m/s. FB: broken by the Forberg blender for 15 min, 30 min, and 70 min. HSM: broken by the laboratory high-speed mixer for 1 min, 2 min, and 7 min.

Highlights

- High-speed mixing and pneumatic conveying caused significant breakage of agglomerated infant formula
- Powder breakage caused increased bulk density and surface free fat
- Powder breakage decreased the rehydration properties of powders, but had only a small influence on powder flowability
- Factory-scale blending had little influence on physical properties of agglomerated infant formula

Table1. Properties of infant formula samples.

Samples	SSA (m^2/kg)	Bulk density (Kg/L)	Particle density (Kg/L)	Porosity (%)	SFF(%)
PC0	$47.6^{c}\pm0.8$	$0.492^{c}\pm0.003$	$1.2571^{b}\pm0.0008$	$55.80^{a}\pm0.08$	$1.183^{b}\pm0.012$
PC40	$51.2^{b}\pm0.8$	$0.506^{b}\pm0.001$	$1.2619^{a}\pm0.0008$	$53.47^{b}\pm0.03$	$1.238^{ab}\pm0.029$
PC50	$55.0^{a}\pm0.3$	$0.517^{a}\pm0.001$	$1.2627^{a}\pm0.0053$	$52.50^{c}\pm0.02$	$1.308^{a}\pm0.001$
FB0	$42.0^{a}\pm0.7$	$0.532^{b}\pm0.003$	$1.2119^{c}\pm0.0004$	$50.89^{a}\pm0.03$	$0.460^{d}\pm0.018$
FB15	$40.2^{ab}\pm0.9$	$0.532^{b}\pm0.005$	$1.2199^{a}\pm0.0007$	$50.30^{b}\pm0.03$	$0.503^{c}\pm0.001$
FB30	$39.0^{b}\pm0.4$	$0.541^{ab}\pm0.009$	$1.2125^{c}\pm0.0002$	$50.87^{a}\pm0.11$	$0.569^{b}\pm0.004$
FB70	$42.3^{a}\pm1.5$	$0.555^{a}\pm0.006$	$1.2185^{b}\pm0.0005$	$48.81^{c}\pm0.12$	$0.645^{a}\pm0.003$
HSM0	$42.0^{d}\pm0.7$	$0.532^{c}\pm0.003$	$1.2119^{d}\pm0.0004$	$50.89^{a}\pm0.03$	$0.460^{d}\pm0.018$
HSM1	$54.8^{c}\pm0.8$	$0.580^{b}\pm0.007$	$1.2203^{c}\pm0.0003$	$45.64^{b}\pm0.15$	$0.947^{c}\pm0.019$
HSM2	$62.6^{b}\pm1.3$	$0.586^{b}\pm0.006$	$1.2285^{b}\pm0.0005$	$45.15^{c}\pm0.06$	$1.233^{b}\pm0.039$
HSM7	$91.8^{a}\pm0.6$	$0.600^{a}\pm0.005$	$1.2311^{a}\pm0.0004$	$44.88^{c}\pm0.14$	$1.884^{a}\pm0.041$

1. PC: broken by pneumatic conveying under the air velocity of 40 m/s and 50 m/s. FB: broken by the Forberg blender for 15 min, 30 min, and 70 min. HSM: broken by the laboratory high-speed mixer for 1 min, 2 min, and 7 min.
2. Values are mean ± standard deviation (n=3).
3. $^{a\text{-}d}$ different values within columns in each group (PC, FB and HSM) are significantly different at $P<0.05$.

Table 2. Loose specific bulk volume and compressibility index of infant formula samples.

Samples	Loose specific bulk volume (L/kg)	*CI* (%)
PC0	$2.031^{a}\pm0.001$	$25.8^{a}\pm0.7$
PC40	$1.976^{b}\pm0.003$	$27.6^{a}\pm0.4$
PC50	$1.934^{c}\pm0.005$	$26.5^{a}\pm0.1$
FB0	$1.88^{a}\pm0.01$	$26.5^{a}\pm0.8$
FB15	$1.88^{a}\pm0.02$	$28.3^{a}\pm2.9$
FB30	$1.85^{a}\pm0.03$	$28.4^{a}\pm2.1$
FB70	$1.80^{b}\pm0.02$	$28.9^{a}\pm0.3$
HSM0	$1.88^{a}\pm0.01$	$26.5^{a}\pm0.8$
HSM1	$1.72^{b}\pm0.02$	$25.6^{a}\pm0.1$
HSM2	$1.71^{bc}\pm0.02$	$29.3^{a}\pm0.2$
HSM7	$1.67^{c}\pm0.01$	$24.7^{a}\pm0.3$

1. PC: broken by pneumatic conveying under the air velocity of 40 m/s and 50 m/s. FB: broken by the Forberg blender for 15 min, 30 min, and 70 min. HSM: broken by the laboratory high-speed mixer for 1 min, 2 min, and 7 min.
2. Values are mean ± standard deviation (n=3).
3. $^{a\text{-}c}$ different values within columns in each group (PC, FB and HSM) are significantly different at $P<0.05$.